IEEE Open Journal of the
Industrial Electronics Society

Received 12 March 2025; revised 28 April 2025; accepted 14 May 2025. Date of publication 22 May 2025;
date of current version 4 June 2025. The review of this article was arranged by Associate Editor L. Ge.

*Digital Object Identifier 10.1109/OJIES.2025.3572372*

# Estimation of the Double-Cage Model for Three-Phase Induction Machines Using Decision Tree-Based Algorithms

**EDUARDO FERREIRA RIOS OLIVEIRA [1], RAFAEL SANTOS [1] (Member, IEEE), MARCELO GODOY SIMÕES [2] (Fellow, IEEE), AND HELMO MORALES PAREDES [1] (Senior Member, IEEE)**

[1]Institute of Science and Technology, São Paulo State University (UNESP), Sorocaba, São Paulo 18087-180, Brazil
[2]Department of Electrical Engineering, School of Technology and Innovations, University of Vaasa, FI-65101 Vaasa, Finland

CORRESPONDING AUTHOR: RAFAEL SANTOS (e-mail: rafael.santos1994@unesp.br).

This work was supported by São Paulo Research Foundation (FAPESP), and the article processing charge for the publication of this work was supported by the Coordenacao de Aperfeicoamento de Pessoal de Nivel Superior (CAPES), Brazil (ROR identifier: 00x0ma614).

**ABSTRACT** This article presents a novel methodology for estimating the double-cage model (DCM) for three-phase induction machines (TIMs) using decision tree-based algorithms. Validated on a diverse dataset of 860 machines spanning a power range from 0.12 to 370 kW, the proposed method stands out by requiring fewer input parameters than traditional techniques like the modified Newton method. Moreover, the proposed approach remains effective even when the input data exhibits statistical deviations, a common challenge in practical scenarios. The main contributions of this work are the reduction of the number of parameters necessary for the estimation of the DCM equivalent circuit and employing three distinct decision tree-based algorithms, whose effectiveness was confirmed through simulations and experimental tests, thereby providing an accurate representation of the dynamics of real TIMs. The results indicate that by using only basic and readily available data from machine nameplates, such as nominal current, power, speed, voltage, and torque, the proposed methodology provides a reliable and efficient framework for incorporating the real dynamics of TIMs into computational models.

**INDEX TERMS** Decision tree algorithms, double-cage model (DCM), induction machines, parameter estimation.

## I. INTRODUCTION

Three-phase induction motors (TIMs) are widely recognized for their compact design, durability, and ease of manufacture, which make them highly preferred for a variety of applications such as pump systems, fans, elevators, and milling equipment. Their widespread use and significant energy consumption have established TIMs as a predominant load in many global electrical infrastructures [1].

A critical area of TIM research is the development of models that accurately capture their dynamic behavior to improve design, optimize control strategies, and enhance diagnostic methods. Various modeling approaches have been proposed in the literature, including physical models [2], finite element method models [3], magnetic equivalent circuit models [4], and models based on Fourier analysis [5]. Among these, lumped parameter models based on equivalent circuits are extensively utilized because of their simplicity and clear physical interpretation. In particular, double-cage models (DCM) are useful for accurately predicting TIM starting current and torque based on the machine manufacturer data, even when various rotor geometries are present [6]. Fig. 1 depicts the DCM single-phase circuit, where $R_1$ and $X_1$ represent the equivalent resistance and inductive reactance of the stator winding, $X_m$ denotes the magnetizing reactance, and $R'_2$, $X'_2$, $R''_2$, and $X''_2$ correspond to the parameters of the inner and outer cages, respectively.

The estimation of DCM parameters can be significantly improved by employing computational techniques that overcome the limitations of experimental methods, especially for high-power TIMs [7]. Techniques such as Newton–Raphson, Levenberg–Marquardt, Damped Newton–Raphson, and genetic algorithms have been applied in this context [8].

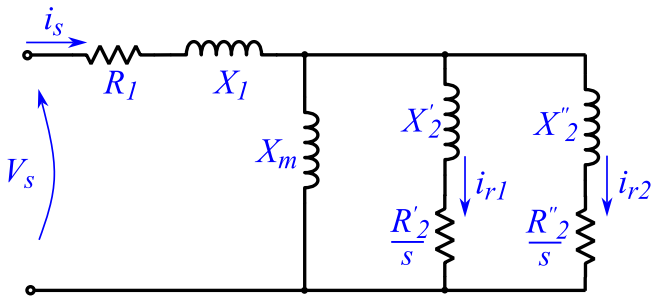


**FIGURE 1.** Double-cage single-phase equivalent circuit for TIM.

However, modified Newton-based approaches are particularly sensitive to errors in the input data arising from statistical deviations, since manufacturers typically provide values within the tolerances allowed by the IEC standards [9], which can lead to inaccuracies in the estimated equivalent circuit parameters [10]. Although the method described in [6], [10] provides accurate estimates when provided with well-defined input data, it is limited in practical applications where data variability is common, although it has been integrated into widely used engineering tools such as MATLAB/Simulink [11].

Recently, machine learning (ML) techniques have emerged as a promising alternative to analyze TIM behavior by identifying complex nonlinear patterns without the need for explicit mathematical modeling. Although traditional techniques for motor parameter estimation are based on laboratory no-load and blocked-rotor tests or analytical modeling frameworks, which can be complex, impractical, or time consuming, ML-based methods offer a data-driven alternative that addresses these limitations by allowing scalable, automated, and high-throughput parameter estimation from readily available sources, such as manufacturer catalog or real-time sensor data [12]. Furthermore, these methods can offer improved accuracy even when data sets contain statistical deviations and errors [13]. As can be seen in the recent literature, ML techniques have demonstrated significant potential in the estimation of induction machine parameters. Recent studies illustrate various approaches, including artificial neural networks (ANNs) applied to large motor data sets with reduced error margins [14], genetic algorithms optimized for fault conditions in multiphase systems [15], and hybrid metaheuristic ML methods that improve accuracy and convergence of the estimation [16]. Further advances include ANN models with minimal root mean square errors in broad power ranges [17] and combined evolutionary local search strategies to extract parameters from nameplate data [18].

Collectively, these approaches highlight the applicability of ML to parameter estimation in different motor configurations and operational scenarios, even when noise and nonlinearity are present. Although several studies have used ANNs for parameter estimation, decision trees (DT) are often preferred for tabular datasets due to their superior interpretability, simpler architecture, fewer hyperparameters and generally faster classification times [19]. Despite these advantages, few works in the literature have explored the use of DTs to estimate equivalent TIM circuit parameters, particularly within the context of the DCM.

In this context, the primary objective of this article is to enhance the modified Newton method presented in [10] by proposing a novel TIM parameter estimation approach for the DCM that employs DT algorithms, applicable to machines with power ratings up to 370 kW, operating under normal, fault-free conditions. The proposed methodology offers several key advantages, including the use of a reduced number of input parameters and the demonstration of robustness to lower-quality statistical input data while still achieving accurate DCM parameter estimates. This is accomplished by constructing a dataset of over 860 TIMs using MATLAB's "power AsynchronousMachineParams" function, and then employing three DT algorithms, XGBoost, CatBoost, and Random Forest, to estimate the various DCM circuit parameters. The effectiveness of the proposed methodology is validated through both simulations and experimental tests.

The main contributions of this work are as follows.

1) A reduction in the number of input parameters required for determining DCM equivalent circuit parameters, as compared to the modified Newton method.
2) The implementation and validation of three distinct DT algorithms for estimating DCM equivalent circuit parameters.
3) An assessment comparing the proposed method with conventional techniques under conditions of input data variability, demonstrating superior performance.

The rest of this article is organized as follows. Section II discusses the DCM and the modified Newton method. Section III presents the DT algorithms (XGBoost, CatBoost, and Random Forest) used in this work. Section IV details the construction and preprocessing of the TIM dataset. Section V focuses on model hyperparameter optimization and evaluation metrics. Section VI presents the simulated and experimental results. Finally, Section VII concludes this article.

## II. DOUBLE-CAGE INDUCTION MOTOR MODEL

The structure of the TIM consists of a stator and a rotor. The rotor is typically of the squirrel-cage type and can feature various bar geometries. These variations result in different lumped-parameter circuit models, such as single-cage and double-cage configurations. The double-cage model offers distinct characteristics and advantages for specific applications, and its equivalent circuit model provides a more precise description of torque and current characteristics compared to single-cage models [20], [21]. For this reason, the DCM formulation was adopted for TIM.

Fig. 1 presents the equivalent circuit per phase for a double-cage TIM. In this circuit, $V_s$ and $i_s$ denote the voltage and current of the stator phase, respectively. The currents of the inner and outer cages are represented by $i_{r1}$ and $i_{r2}$, respectively. The stator resistance $R_1$ models the energy losses due to the

Joule effect in the stator windings, while the reactance $X_1$ accounts for magnetic flux leakage from the stator windings. For the rotor, the outer cage resistance $R_2''$ accounts for both the energy delivered to the mechanical system and the associated thermal losses, whereas the inner cage resistance is indicated by $R_2'$. The leakage reactances for the inner and outer cages are $X_2'$ and $X_2''$, respectively. In addition, the model incorporates the magnetizing reactance $X_m$, which represents the magnetic flux responsible for generating the rotating magnetic field in the air gap.

### A. MODIFIED NEWTON METHOD TO ESTIMATE DCM OF TIM

The parameters of DCM can be determined by solving a system of six nonlinear equations (1)–(6), using a modified Newton method, as described in [10]. This method relies on common manufacturer data, including nominal mechanical power ($P_N$), nominal power factor ($PF_N$), maximum torque ($T_M$), starting current ($I_{ST}$), starting torque ($T_{ST}$), nominal efficiency ($\eta_N$), and rated slip ($s_N$). A critical aspect of this approach is its requirement for an extensive set of input data. In addition to the aforementioned parameters, the method requires the nominal stator's root mean square (RMS) voltage ($V_n$), the nominal frequency ($f_n$), nominal current ($I_n$), nominal mechanical torque ($T_n$), nominal speed ($N_n$), synchronous speed ($N_s$), as well as several torque and current ratios, such as the starting current to nominal current, starting torque to nominal torque, and breakdown torque to nominal torque ratios. With these inputs, the parameters $R_1, X_1, X_m, R_2', X_2', R_2'$, and $X_2''$ can be easily calculated using MATLAB/Simulink's "power_AsynchronousMachineParams" function.

$$f_1(x) = \frac{P_N - P(s_N)}{P_N} = 0 \tag{1}$$

$$f_2(x) = \frac{PF_N - PF(s_N)}{PF_N} = 0 \tag{2}$$

$$f_3(x) = \frac{T_M - T(s_M)}{T_M} = 0 \tag{3}$$

$$f_4(x) = \frac{I_{ST} - I(1)}{I_{ST}} = 0 \tag{4}$$

$$f_5(x) = \frac{T_{ST} - T(1)}{T_S T} = 0 \tag{5}$$

$$f_6(x) = \frac{\eta_N - \eta(s_N)}{\eta_N} = 0. \tag{6}$$

However, the accuracy of this method is highly dependent on the precise determination of input parameters. This dependence highlights the statistical sensitivity of the method and underscores the need for reliable data to ensure accurate predictions of motor performance. In addition, the large number of inputs required can complicate practical applications, as obtaining consistent and precise measurements is not always feasible in real-world scenarios. In some cases, the TIM datasheet may be unavailable or may not provide all the necessary data.

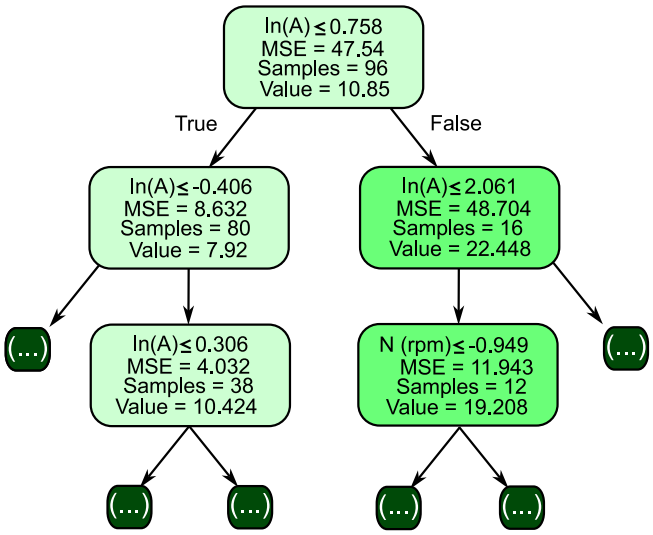


**FIGURE 2.** Partial visualization of a Random Forest DT for predicting $X_m$.

## III. DECISION TREE-BASED ALGORITHMS

DT-based algorithms are widely employed in various fields, including classification, regression, and feature selection [22]. Their fundamental concept involves recursively partitioning the data into subsets based on attribute values until a stopping criterion is reached, resulting in a tree structure where each node represents a decision based on a specific attribute. The optimal attribute for each split is selected using criteria such as information gain, gain ratio, and Gini index [23]. An important advantage of DTs is their interpretability, enabling users to easily understand and explain the decision-making process [24]. In addition, these algorithms effectively handle both categorical and numerical data, enhancing their versatility and efficiency across a wide range of applications.

In this context, DT-based algorithms are selected in this work due to their interpretability, computational simplicity, and suitability for tabular data [25], which generally characterize motor nameplate information. Moreover, its transparency and traceability features facilitate the analysis of the influence of input variables, such as voltage, current, speed, and torque, in the estimation of the DCM parameters [26]. Moreover, DTs are also robust to incomplete or noisy inputs, maintaining consistent performance even under data statistical deviations [27], which is a common scenario in practice. Furthermore, DTs can capture nonlinear dependencies between features without requiring intensive data preprocessing [28], allowing direct modeling of the complex relationships inherent in the estimation of DCM parameters. In addition, DT exhibits greater efficiency in scenarios involving smaller datasets [29].

Fig. 2 depicts a partial representation of how the Random Forest DT is applied in this work to predict $X_m$, for example. In this example, each node represents a conditional split, where the dataset is divided based on the most influential features to minimize the Mean Squared Error (MSE). The primary splitting criterion in this case is the nominal current ($I_n$ [A]),

**Algorithm 1:** Gradient Boosting.

**Input:** Dataset $\mathcal{D}$
Loss Function $L$
Base Learner $\mathcal{L}_\phi$
Number of Iterations $M$
Learning Rate $\eta$
Initialize the model:

$$F^{(0)}(x) = \arg\min_{\theta} \sum_{i=1}^{n} L(y_i, \theta)$$

**for** $m = 1$ ***to*** $M$ **do**
Compute residuals (negative gradients):

$$\hat{g}_m(x_i) = \left[\frac{\partial L(y_i, F(x_i))}{\partial F(x_i)}\right]_{F(x)=F^{(m-1)}(x)}$$

Fit a new base learner $\phi_m(x)$ by minimizing:

$$\phi_m = \arg\min_{\phi} \sum_{i=1}^{n} [-\hat{g}_m(x_i) - \beta\phi(x_i)]^2$$

Compute the weight $\rho_m$:

$$\rho_m = \arg\min_{\rho} \sum_{i=1}^{n} L(y_i, F^{(m-1)}(x_i) + \rho\phi_m(x_i))$$

Update the model:

$$F^{(m)}(x) = F^{(m-1)}(x) + \eta\rho_m\phi_m(x)$$

**Output:** Final model:

$$F(x) \equiv F^{(M)}(x) = \sum_{m=1}^{M} \eta\rho_m\phi_m(x)$$

indicating its strong influence on the prediction of $X_m$. Further down the tree, additional features, such as the nominal speed ($N$ [RPM]), refine the predictions by progressively dividing the data.

### A. GRADIENT BOOSTING

While DTs are powerful models, they often suffer from overfitting and limited predictive performance when used individually [30]. Ensemble methods, such as Boosting, overcome these limitations by combining multiple weak learners into a strong predictive model. In Boosting, DTs are trained sequentially, with each tree correcting the errors of its predecessor and thereby refining the overall model. Among the various Boosting techniques, Gradient Boosting stands out as one of the most effective approaches, as it iteratively minimizes prediction errors through gradient-based optimization [31]. Gradient Boosting follows an iterative approach to minimize prediction errors by sequentially improving the model. The process begins with an initial prediction, $F^{(0)}(x)$, chosen to minimize the overall loss function. In each iteration, the algorithm focuses on the residual errors, computed as the negative gradients of the loss function relative to the current predictions, and then trains a new weak model, $\phi_m(x)$, to approximate these residuals. To achieve optimal correction, the algorithm determines an optimal weight, $\rho_m$, which minimizes the loss when $\phi_m(x)$ is added to the existing model. Here $\eta$ represents the learning rate that controls the contribution of each new model. This iterative process, repeated for $M$ iterations, progressively improved the model's accuracy, as outlined in Algorithm 1.

### B. XGBOOST, CATBOOST AND RANDOM FOREST

XGBoost employs gradient boosting techniques that combine high predictive performance with computational efficiency. A key advantage of XGBoost is its robustness against overfitting, achieved through built-in regularization that constrains model complexity and promotes better generalization to unseen data [32]. By penalizing overly complex models, XGBoost maintains a balance between accuracy and simplicity, enhancing its overall predictive capabilities. In contrast, CatBoost (Categorical Boosting) is a gradient boosting algorithm specially designed for classification and regression tasks. A key feature of CatBoost is its built-in overfitting detector, which can stop the training earlier when excessive model complexity is detected, thereby improving the model's performance and reliability [33]. Furthermore, CatBoost uses ordered boosting to prevent target leakage from influencing model predictions [34]. These mechanisms enable CatBoost to deliver robust and accurate predictions for parameters like $X_1$ and $X_2'$. Moreover, Random Forest is an ensemble learning method based on bagging (Bootstrap Aggregating), where multiple DTs are trained independently on random subsets of the data. Unlike boosting, which builds trees sequentially to correct previous errors, bagging trains each tree in parallel and then combines their predictions, typically by averaging them in regression tasks [35]. This approach reduces the risks of overfitting individual trees.

## IV. DATA COLLECTION AND PREPROCESSING

The dataset utilized in this work was constructed with MATLAB's "power_AsynchronousMachineParams" function available in MATLAB/Simulink, which employs the mathematical procedure described in Section II-A to determine the seven circuit parameters ($R_1$, $X_1$, $X_m$, $R_2'$, $X_2'$, $R_2''$ and $X_2''$). Data were compiled from multiple manufacturers' catalogs to ensure a diverse representation of TIM. In total, specifications for 860 TIMs were collected, covering power ratings from 0.12 kW to 370 kW. During dataset construction, TIMs with outlier circuit parameters or high estimation errors were excluded. Table 1 provides examples of specifications of TIM's M1–M4, which are present in the utilized dataset. Furthermore, the dataset underwent pre-processing before training and classification to enhance the model's robustness against variations in input data.

The proposed model relies on key electrical parameters of TIMs while significantly reducing the number of input variables compared to the method proposed in [10]. In this work, the selected inputs are the nominal line current ($I_n$

**TABLE 1. Examples of TIM Specifications From Manufacturer Data**

| Manufacturer Specifications | | | | | | | | | | |
|---|---|---|---|---|---|---|---|---|---|---|
| TIM | $V_n$ **[V]** | $f_n$ **[Hz]** | $P$ **[kW]** | $I_n$ **[A]** | $T_n$ **[Nm]** | $N$ **[RPM]** | $I_s/I_n$ | $T_s/T_n$ | $T_b/T_n$ | $PF$ |
| M1 | 460 | 60 | 7.5 | 12.4 | 40 | 1770 | 9.6 | 2.7 | 4.2 | 0.83 |
| M2 | 460 | 60 | 15 | 26 | 122 | 1178 | 6.8 | 2.5 | 3 | 0.79 |
| M3 | 460 | 60 | 22 | 37.5 | 178 | 1180 | 6.3 | 2.6 | 2.8 | 0.79 |
| M4 | 460 | 60 | 90 | 142 | 721 | 1192 | 7.7 | 2.7 | 3 | 0.84 |

[A]), the nominal power ($P$ [kW]), the nominal speed ($N$ [RPM]), the nominal voltage ($V_n$ [V]), and the nominal torque ($T_n$ [Nm]). This choice was motivated by the feasibility and the satisfactory results obtained during the tests, enhancing the approach's suitability for practical applications. This reduction in the input features was achieved through feature engineering [36] and transformation methods [37]. The selection of transformation techniques was based on empirical evaluations of their impact on model performance, specifically evaluated using MSE metrics. For example, reciprocal transformations, represented by $f(x) = \frac{1}{x}$, effectively normalize extreme values [38], and significantly reduce the MSE for the parameter $R_1$. In contrast, the $R_2''$ parameter showed improved performance when an advanced transformation, combining polynomial and interaction features, was applied. For the remaining parameters, no transformation was necessary, suggesting that their relationship with the inputs was already sufficiently linear or that additional transformations would introduce unnecessary complexity. Overall, this feature engineering approach enabled the model to maintain reliable predictions even when input conditions vary, thereby increasing its applicability in practical scenarios.

## V. MODEL TRAINING AND VALIDATION

The training process involved fitting the models to transformed data and evaluating their performance using both the MSE and Shapley additive explanations (SHAP) values [39], which provide insight into the contributions of features to the predictions. To optimize the performance of the model, an open-source hyperparameter optimization framework [40] was employed to fine-tune the parameters of each model using a tree-structured Parzen estimator (TPE) algorithm [41]. This approach systematically explored and refined hyperparameter combinations, such as the number of estimators, maximum tree depth, and the minimum number of samples required to split a node. After 50 tests, the best-performing set of hyperparameters was selected to train the final model. The three algorithms, XGBoost, CatBoost, and Random Forest, were rigorously evaluated for each output parameter.

## VI. RESULTS

This section presents the main results obtained from exploring the following aspects: the estimation accuracy of DCM parameters, the robustness of the system to input variations, and the experimental results.

### A. PARAMETER ESTIMATION ACCURACY

The final model was evaluated on a subset of 50 TIMs, with the motors described in Table 1 serving as a representative sample covering ranging from 7.5 to 90 kW. Fig. 3 shows the values for the circuit parameters ($R_1$, $X_1$, $X_m$, $X_2'$, $R_2'$, $X_2''$ and $R_2''$) obtained using the Modified Newton method (as detailed in Section IV) alongside the values estimated using different DT algorithms that require only five inputs parameters. Specifically, the XGBoost algorithm was employed to estimate $R_1$, $R_2'$, and $R_2''$; CatBoost was used for $X_1$ and $X_2'$; and Random Forest was applied for $X_m$ and $X_2''$. These algorithms were selected through iterative evaluations to achieve optimal performance.

Fig. 3 also indicates the percentage Absolute Relative Error (ARE) between the reference and estimated parameter values. In general, the results show that the discrepancies are minimal for most circuit parameters across TIMs M1 to M4. For $R_1$, $X_1$, $X_2'$ and $R_2''$ the absolute errors were less than 0.5%, while for $R_2'$ and $X_2''$, the errors remained below 2.5%. The highest errors were observed for $X_m$, ranging from 11.035% for TIM M1 to 1.057% for TIM M4.

Fig. 4 compares the electromagnetic torque waveforms for TIMs M1 to M4, using circuit parameter values estimated by both the modified Newton method and the proposed methodology, respectively. Although slight differences are observed between the reference and estimated torque waveforms, these variations are minimal, underscoring the reliability and accuracy of the proposed approach.

### B. ROBUSTNESS TO INPUT VARIATIONS

To assess the efficiency of the proposed method in practical scenarios, where TIM manufacturer data may exhibit statistical deviations, this section examines how both the proposed approach and the modified Newton method respond to small variations in the input parameters.

Fig. 5 shows the DCM circuit parameter estimations for TIM M1 under $V_n$ and $I_n$ variation, with deviations of $\pm 1\%$, $\pm 3\%$, and $\pm 5\%$ for these variables. As shown in Figs. 5(a) and 5(b), the conventional method exhibits significant discrepancies in the estimated parameters when $V_n$ and $I_n$ vary. For example, with a $V_n$ deviation, the conventional method produced an ARE of 44% while the proposed methodology achieved an error of only 4% for $R_1$. Similarly, for deviations in $I_n$, the conventional method yielded an absolute error of 414% for $X_2'$, compared to a 0% error with the proposed approach.

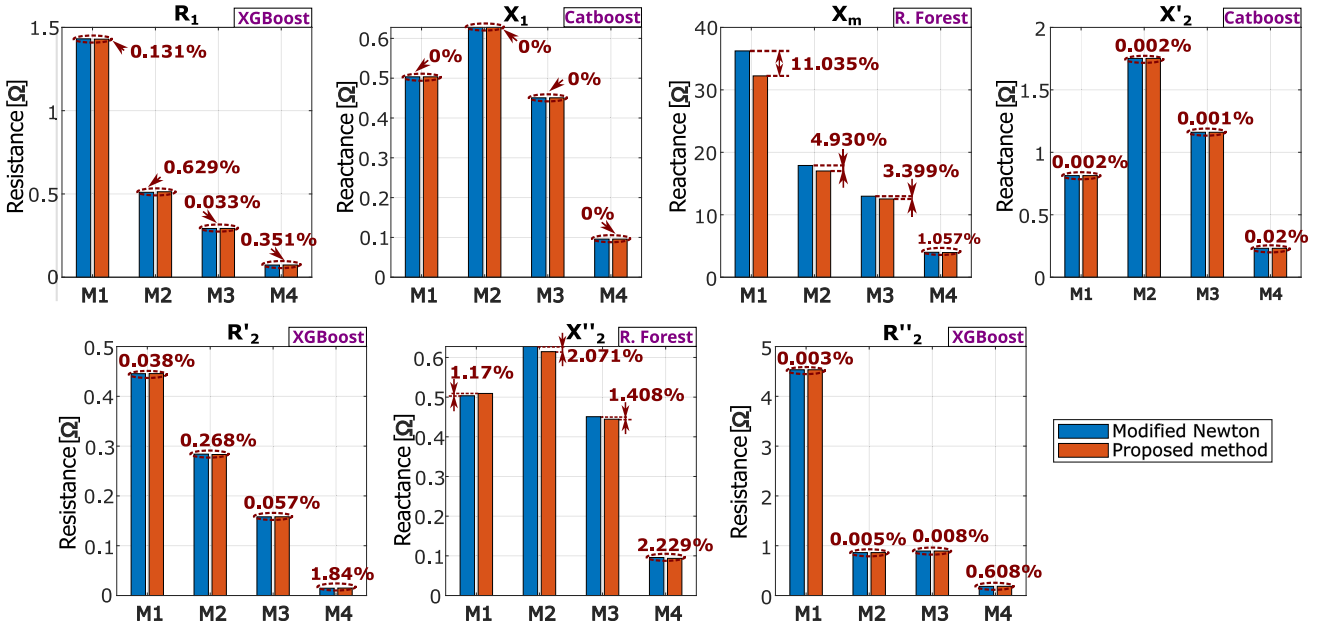


**FIGURE 3.** Estimated DCM circuit parameters, comparing values estimated using the modified Newton and proposed methods.

**TABLE 2.** Standard Deviation of the Absolute Maximum Relative Error ($\sigma_{ARE}$) for Different DCM Parameters Under Different Variations of Input Parameters

| Variation | Method | $\sigma_{ARE}(R_1)$ | $\sigma_{ARE}(X_1)$ | $\sigma_{ARE}(X_m)$ | $\sigma_{ARE}(X'_2)$ | $\sigma_{ARE}(R'_2)$ | $\sigma_{ARE}(X''_2)$ | $\sigma_{ARE}(R''_2)$ | Med($\sigma_{ARE}$) |
|---|---|---|---|---|---|---|---|---|---|
| $N$ | Modified Newton | 50.27 | 105.90 | 5.74 | 28.80 | 420.91 | 105.89 | 26.62 | 50.27 |
| | Proposed | 39.27 | 6.16 | 2.10 | 41.60 | 536.77 | 7.46 | 18.20 | 18.20 |
| $T$ | Modified Newton | 27.30 | 30.98 | 7.04 | 176.48 | 34.94 | 30.98 | 88.71 | 30.98 |
| | Proposed | 40.39 | 33.47 | 1.08 | 55.98 | 3.22 | 13.53 | 22.37 | 22.37 |
| $I_n$ | Modified Newton | 28.22 | 32.04 | 1.28 | 195.01 | 39.94 | 32.04 | 80.81 | 32.04 |
| | Proposed | 6.31 | 9.33 | 5.77 | 17.07 | 5.68 | 10.32 | 69.09 | 9.33 |
| $V_n$ | Modified Newton | 27.57 | 33.67 | 1.16 | 175.99 | 30.06 | 33.67 | 93.43 | 33.67 |
| | Proposed | 8.06 | 9.66 | 4.69 | 13.46 | 11.92 | 1.77 | 10.92 | 9.66 |

Fig. 6 expands the results depicted in Fig. 5 by showing the maximum ARE with input variations: –1%, –3%, –5% for $N$ (Fig. 6(a)); ±5%, ±3%, ±1% for $T$ (Fig. 6(b)); and ±5%, ±3%, ±1% for $V_n$ and $I_n$ [Fig. 6(c), Fig. 6(d)], across four different motors (M1–M4), whose parameters were described in Table 1. This figure considers the parameters obtained usin the modified Newton method [10] and the proposed method.

In overall, it can be observed that a greater number of errors equal to or greater than 100% occurred for the modified Newton method compared to the proposed method. For example, considering variations in $N$, nine cases exhibited errors greater than or equal to 100% under the traditional method, while only three such cases were observed under the proposed method. Similarly, for variations in $T$, five cases exceeded the error of 100% for the traditional method, while only one case did so for the proposed method. In the case of variations in $V_n$, five errors greater than 100% were recorded for the traditional method, while no such errors were observed for the proposed method. Finally, for variations in $I_n$, five instances of errors exceeding 100% were identified using the traditional method, compared to only one instance under the proposed method.

In addition, it is noted that the ARE values for the proposed method tend to be relatively lower for more parameters, even considering different TIM. To better evaluate this last aspect, the standard deviation of the absolute maximum relative error ($\sigma_{ARE}$) was calculated for different variations in input parameters, considering the modified Newton method and the proposed method, as shown in Table 2. As can be seen by the red numbers in Table 2, the proposed method exhibited a lower $\sigma_{ARE}$ than the modified Newton method for variations in $N$ and $T$ in two parameters, namely $X'_2$ and $R'_2$. For the $I_n$ and $V_n$ cases, it had a lower $\sigma_{ARE}$ in only one parameter, $X_m$. To represent the overall behavior of $\sigma_{ARE}$ the median of $\sigma_{ARE}$ was calculated and indicated as Med($\sigma_{ARE}$) in Table 2.

### C. EXPERIMENTAL RESULTS

To validate the proposed methodology for predicting the DCM circuit parameters of a real TIM, experimental tests were performed using a 0.37 kW TIM rated at 1780 r/min. This machine operates in both Δ and Y connections, with line voltages of 220/380 V and line currents of 2.08/1.20 A,

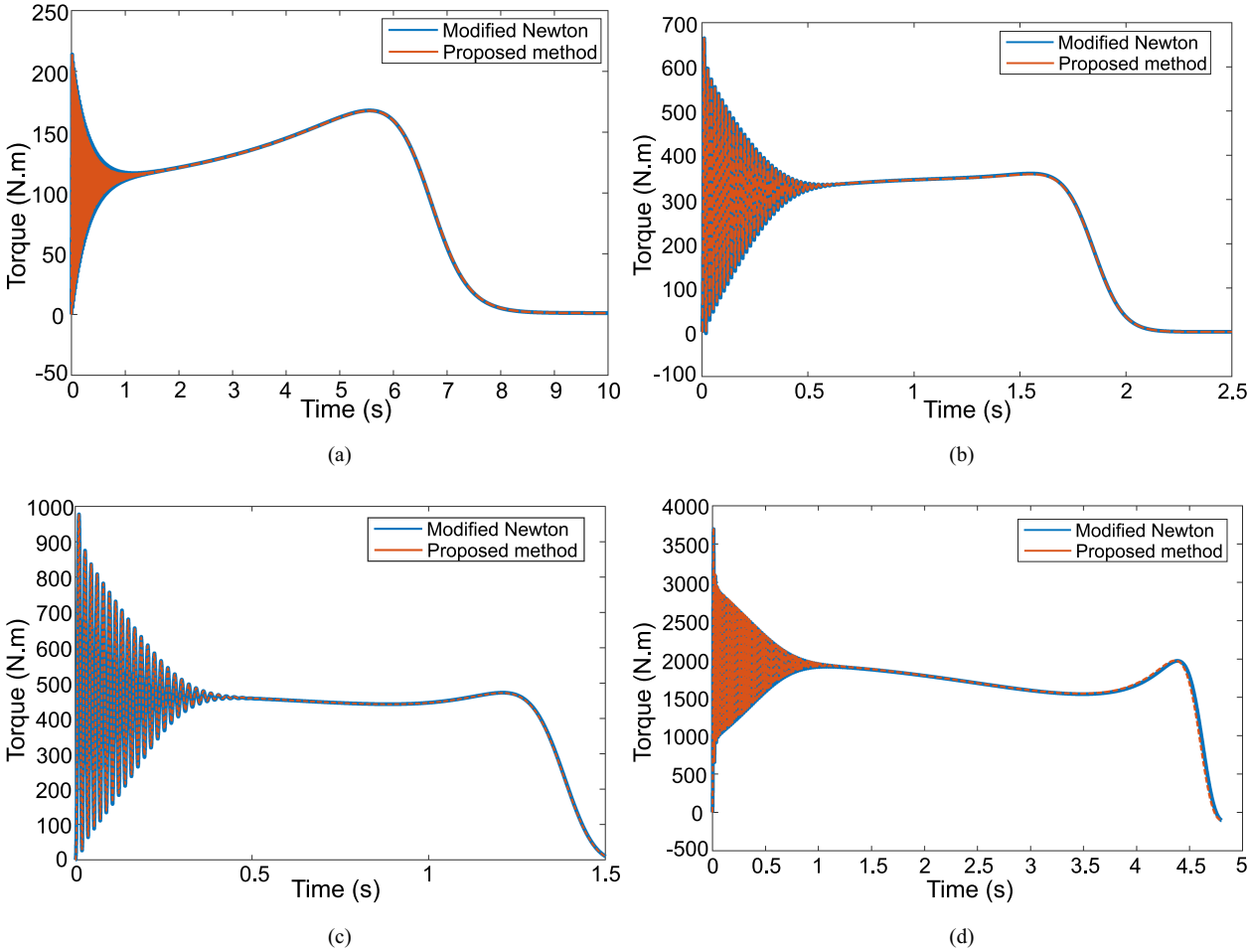


**FIGURE 4.** Electromagnetic torque waveforms for estimated DCM parameters, using the modified Newton and the proposed methods for: (a) M1; (b) M2; (c) M3; (d) M4.

respectively. The TIM's mechanical load was provided by an electromagnetic brake equipped with a load cell, set to deliver a steady-state torque of 0.5 Nm. During the experiment, the TIM was connected in a $\Delta$ configuration, with a manually controlled circuit breaker, mounted on a circuit panel, directly supplying a 220 V line voltage (grid supply). An GMT-P1 sensor was used to measure the angular shaft speed, and its data were transmitted to a host PC via a ModBus serial protocol configured at 9600 Bd with a 1ms response time. Line voltages and currents were measured using two voltage probes and two high-resolution current probes connected to a Tektronix DPO3014 oscilloscope, while stator phase voltages and currents were obtained mathematically. Fig. 7 shows the experimental setup used to validate the proposed methodology.

Fig. 8 compares experimental waveforms with MATLAB simulation results of the TIM model using DCM parameters obtained via the proposed method. For the practical experiment with a 220 V motor line voltage, different DT algorithms were employed: XGBoost to estimate $R_1$, CatBoost to estimate $X_1$, $R_2'$, $X_2''$, and $R_2''$, while RandomForest to estimate $X_m$ and $X_2'$. The resulting DCM parameters for simulation model were: $R_1 = 8.92\ \Omega$, $X_1 = 2.76\ \Omega$, $X_m = 66.91\ \Omega$, $X_2' = 2.87\ \Omega$, $R_2' = 8.13\ \Omega$, $X_2'' = 2.76\ \Omega$, and $R_2'' = 8.23\ \Omega$. For mechanical modeling, an inertia $J$ of 0.00734 kg.m.$^2$ and viscous friction coefficient $B$ of 0.0058 N.m.s/rad were used. The total shaft torque load was calculated as $T_{load} = k\omega^2 + B\omega$, with $k = 3.5854 \times 10^{-6}$ and $\omega$ as angular speed.

Fig. 8(a) illustrates the shaft's angular velocity from both experimental and simulation tests. Both tests show an acceleration period of approximately 0.33 s. In steady-state, the experimental angular velocity reached 1779 RPM, while the simulation produced 1759 RPM, an ARE of 1.12%.

Fig. 8(b) presents the RMS current for stator phase A (with similar results for phases B and C). During start-up, the maximum current values were 9.36 A in the experimental and 9.33 A in the simulation, resulting in an error margin of 0.32%. In steady-state, the RMS current was approximately 1.79 A experimentally versus 1.85 A in the simulation, yielding a 3.3% error. In addition, the instantaneous current values of $I_a$ show a strong agreement between the experimental and simulated results, particularly in the steady-state conditions.

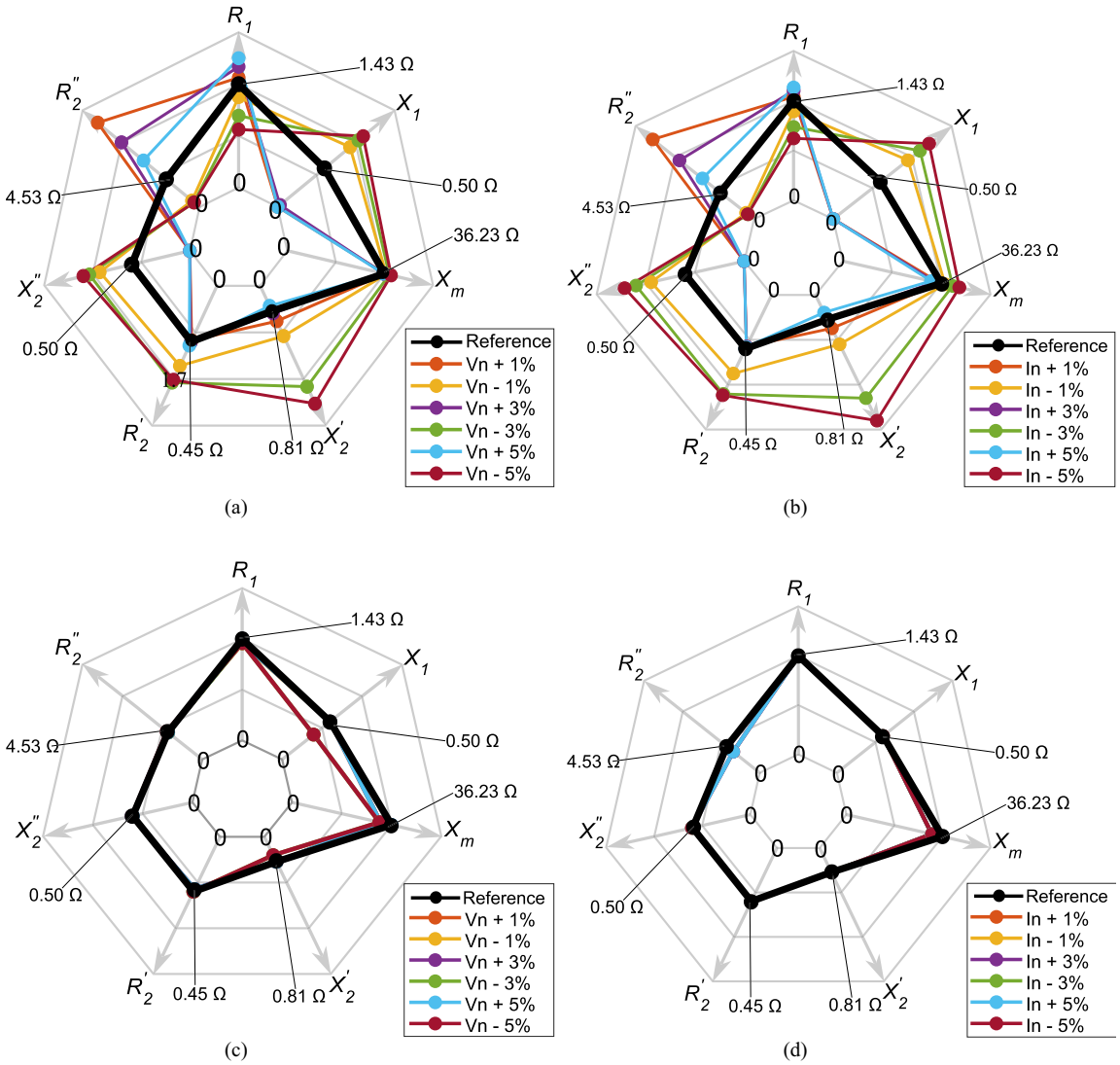


**FIGURE 5.** Radar charts of estimated DCM circuit parameters for variations in $V_n$ and $I_n$, using the modified Newton method–(a) and (b)–and the proposed method–(c) and (d).

Fig. 8(c) compares the active power ($P$) and the reactive power ($Q$) of the TIM during its start-up phase. As expected, both $P$ and $Q$ peak during the transient period. In the practical experiment, the maximum active power reached 3.36 kW, while the simulation produced 3.14 kW, a discrepancy of approximately 6.5%. For reactive power, the experimental value was 2.82 kVAr, whereas the simulation yielded only 1.34 kVAr, representing a larger difference of about 52%. Under steady-state conditions, the experimental measurements were 320 W for $P$ and 627 VAr for $Q$, closely matching the simulation values of 315W and 630 VAr, with differences of just 1.6% and 0.5%, respectively.

Finally, Fig. 8(d) illustrates the progression of the power factor ($PF$) during the start-up process. During the transient period, the experimental $PF$ fluctuates around 0.86, while the simulation showed a slightly higher value around 0.92, a 6.5% difference. In the steady-state, both the experimental and simulated $PF$ stabilized at approximately 0.44, demonstrating strong concordance between the model and the experimental observations.

### D. DISCUSSION

The proposed model demonstrated increased robustness against input parameter deviations compared to the traditional modified Newton method, notably requiring fewer input variables (five instead of seven). For higher power TIMs, typically with a line voltage of 440-460 V, the optimal DT algorithm configuration involved using XGBoost for $R_1$, $R'_2$, and $R''_2$, CatBoost for $X_1$, $X'_2$, and Random Forest for $X_m$ and $X''_2$ . In contrast, tests on a 0.37 kW TIM operating at 220 V required a different configuration: XGBoost was used for $R_1$, CatBoost for $X_1$, $R'_2$, $X''_2$, $R''_2$ and Random Forest for $X_m$ and $X'_2$. This variability in the use of algoritm types seems to indicate that

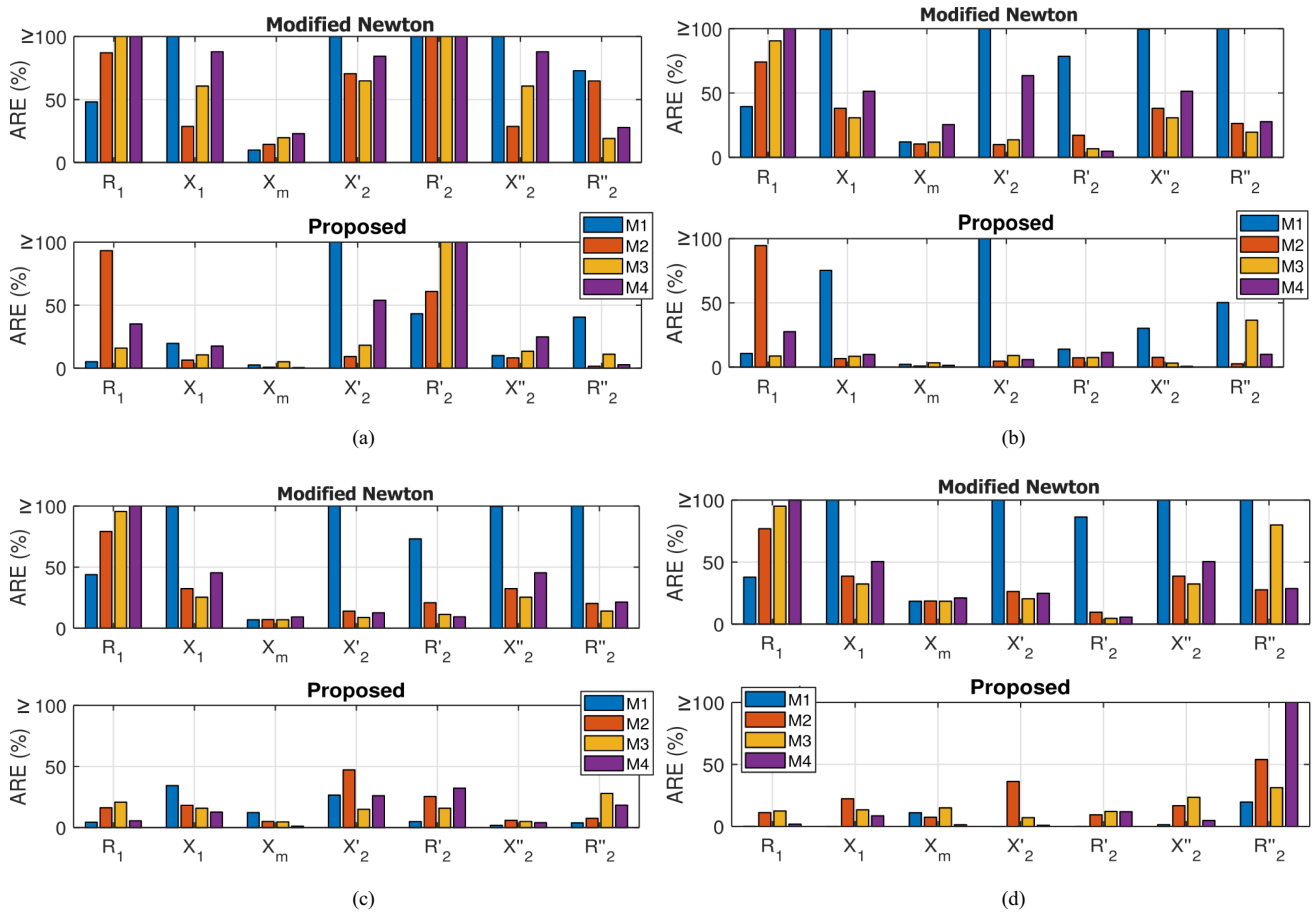


**FIGURE 6.** Maximum Absolute relative error (ARE) obtained for different TIM DCM parameters under variation of distinct input parameters: (a) $N$; (b) $T$; (c) $V_n$ and (d) $I_n$.

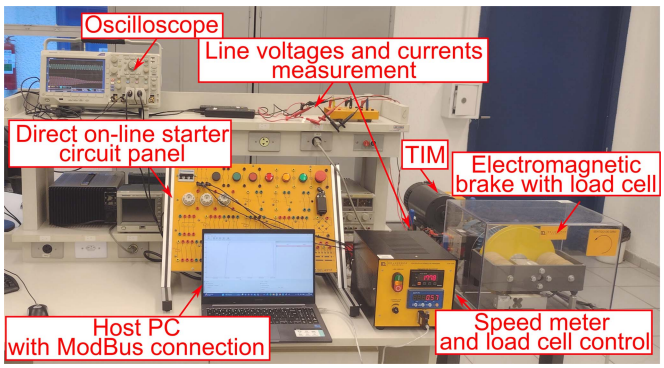


**FIGURE 7.** Experimental setup.

no single DT algorithm is universally optimal for estimating all DCM circuit parameters across different power levels.

Despite some discrepancies with parameters derived from modified Newton method (as shown in Fig. 4), the proposed method effectively identified key parameters governing TIM dynamics. Fig. 5 further demonstrates that, unlike the traditional method, which is highly sensitive to statistical variations in input parameters, the proposed method efficiently handles such variations. This capability is crucial for practical TIM parameter estimation, where manufacturer datasheets often exhibit statistical deviations and data may be limited.

Furthermore, as can be observed in Table 2, when the proposed method performed poorly compared to the modified Newton metho, it was in relation to variations of critical input parameters, such as $N$ and $T$. Although the maximum ARE were greater for the modified Newton method for the parameters $X_2'$ and $R_2'$ ($N$ input variation) and $R_1$ and $X_1$ ($T$ input variation), as can be seen from Fig. 6, the magnitude of the errors tended to remain similar between different machines. In contrast, for the proposed method, while the errors could be low for certain machines, they could become significantly higher for others, indicating greater $\sigma_{ARE}$. However, to properly evaluate the robustness of the proposed method in general, it is important to note that using the mean of $\sigma_{ARE}$ may not be appropriate, as outliers heavily influence the average; therefore, the median provides a more robust measure. In general, the median values of $\sigma_{ARE}$ for the proposed method, compared to the modified Newton method, as shown in Table 2 indicates that, with the proposed method, the estimated parameters tend to remain closer to the original values even under different parametric variations and different TIMs, which is consistent with the behavior illustrated in Fig. 5

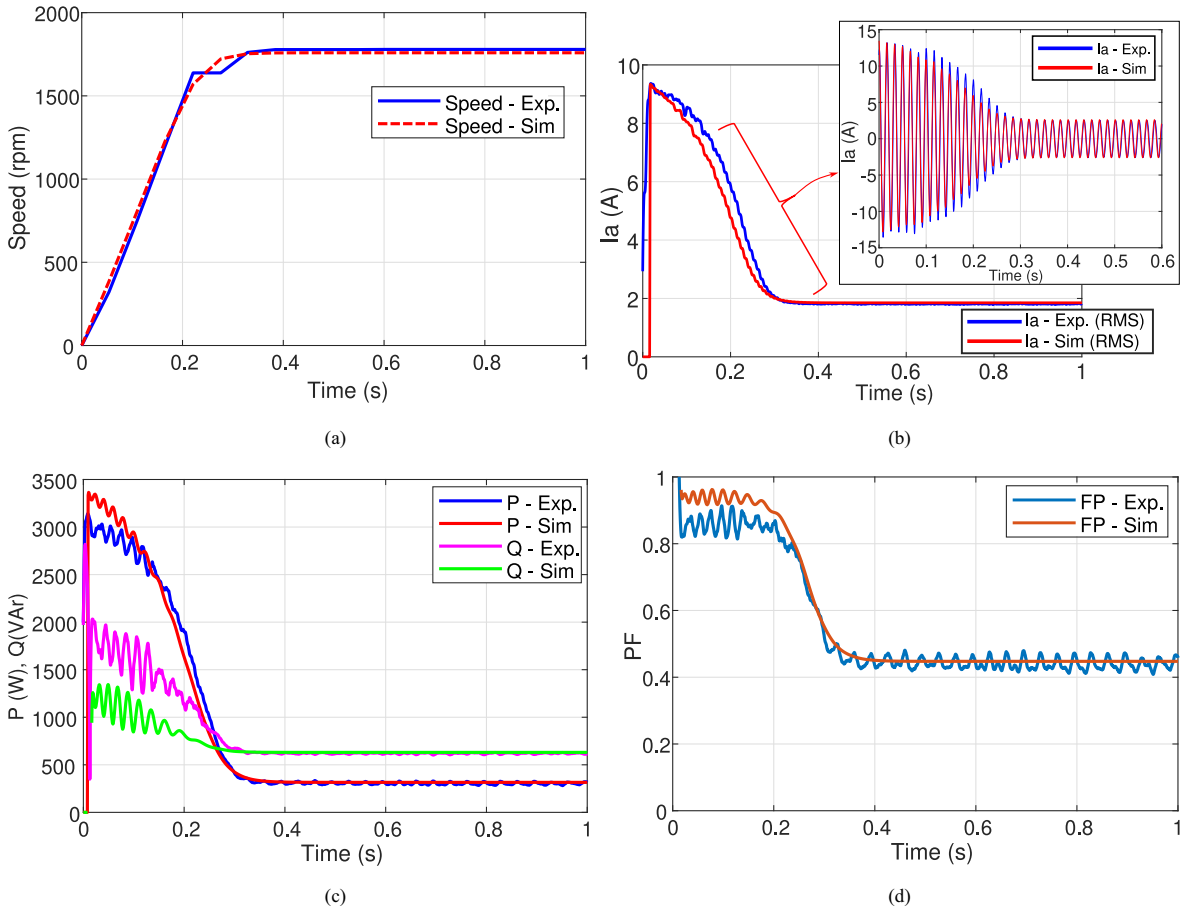


**FIGURE 8.** **Experimental and Simulation waveforms for: (a) Rotor angular speed (r/min); (b) A-phase Stator current (RMS and instantaneous); (c) Active and Reactive Power; d) Power Factor.**

and indicates the robustness and stability of the proposed approach.

Moreover, as illustrated in Fig. 8 the proposed method effectively estimates the DCM parameters of a real TIM, yielding excellent agreement between experimental and simulated waveforms. These findings imply that, by using basic inputs such as nominal line current $I_n$ [A], nominal power $P$ [kW], nominal speed $N$ [RPM], nominal voltage $V_n$ [V], and nominal torque $T_n$ [Nm], parameters commonly found on TIM rating plates, the proposed methodology can reliably capture the dynamics of real TIMs in computational models.

## VII. CONCLUSION

This article proposed a novel methodology for estimating the DCM parameters of TIMs using three DT-based algorithms. The proposed approach has demonstrated accuracy and robustness in both simulations and experimental tests, effectively capturing the dynamic behavior of TIMs. A key contribution of this work is the development of an alternative, more efficient estimating technique for DCM circuit parameters which require fewer input parameters. This method is particularly advantageous for industrial designs and control systems, as it simplifies data requirements and effectively handles scenarios where input data exhibits statistical deviations. The results demonstrate considerable practical potential, though further validation across a wider range of TIM ratings is advised. Future research will focus on applying this methodology to machines with varying ratings, further enhancing its applicability and robustness.

## REFERENCES

[1] D. F. de Souza, F. A. M. Salotti, I. L. Sauer, H. Tatizawa, A. T. de Almeida, and A. G. Kanashiro, "A performance evaluation of three-phase induction electric motors between 1945 and 2020," *Energies*, vol. 15, no. 6, 2022, Art. no. 2002.

[2] S. Mojlish, N. Erdogan, D. Levine, and A. Davoudi, "Review of hardware platforms for real-time simulation of electric machines," *IEEE Trans. Transport. Electrific.*, vol. 3, no. 1, pp. 130–146, Mar. 2017.

[3] A. Zhao, H. Chen, C. Boßer, and M. Leksell, "FEM and CFD thermal modeling of an axial-flux induction machine with experimental validation," *Case Stud. Thermal Eng.*, vol. 53, 2024, Art. no. 103879.

[4] B. D. S. G. Vidanalage, A. Lombardi, J. Tjong, and N. C. Kar, "Magnetic field-based induction machine modeling incorporating space and time harmonic effects," *IEEE Access*, vol. 12, pp. 41579–41589, 2024.

[5] J. Li, L. Wu, and X. Wu, "Advanced computational-time reduction technology of nonlinear fourier-based and magnetic circuit hybrid model," *IEEE Trans. Transport. Electrific.*, vol. 11, no. 1, pp. 3617–3630, Feb. 2025.

[6] J. Pedra and F. Corcoles, "Estimation of induction motor double-cage model parameters from manufacturer data," *IEEE Trans. Energy Convers.*, vol. 19, no. 2, pp. 310–317, Jun. 2004.
[7] M. O. Gülbahçe and M. E. Karaaslan, "Estimation of induction motor equivalent circuit parameters from manufacturer's datasheet by particle swarm optimization algorithm for variable frequency drives," Istanbul University, 2022.
[8] J. Susanto and S. Islam, "Improved parameter estimation techniques for induction motors using hybrid algorithms," 2017, *arXiv:1704.02424*.
[9] N. Nilsson, "A comparison of ansi and iec standards for power station polyphase induction (asynchronous) motors," *IEEE Trans. energy Convers.*, vol. 11, no. 3, pp. 500–507, Sep. 1996.
[10] J. Pedra, "On the determination of induction motor parameters from manufacturer data for electromagnetic transient programs," *IEEE Trans. Power Syst.*, vol. 23, no. 4, pp. 1709–1718, Nov. 2008.
[11] MathWorks, "Asynchronous machine parameters," 2023, Accessed: Oct. 15, 2023. [Online]. Available: https://www.mathworks.com/help/sps/powersys/ref/power_asynchronousmachineparams.html
[12] S. Zhang, O. Wallscheid, and M. Porrmann, "Machine learning for the control and monitoring of electric machine drives: Advances and trends," *IEEE Open J. Ind. Appl.*, vol. 4, pp. 188–214, 2023.
[13] M. Drakaki, Y. L. Karnavas, I. A. Tziafettas, V. Linardos, and P. Tzionas, "Machine learning and deep learning based methods toward industry 4.0 predictive maintenance in induction motors: State of the art survey," *J. Ind. Eng. Manage.*, vol. 15, no. 1, pp. 31–57, 2022.
[14] G. Lourenço, G. T. de Arruda, V. E. C. de La Rosa, M. F. Castoldi, A. Goedtel, and W. A. de Souza, "Three-phase induction motor electrical parameter estimation using artificial neural networks," in *Proc. 2024 IEEE Int. Symp. Power Electron., Elect. Drives, Automat. Motion*, 2024, pp. 883–888.
[15] A. M. Fadel, A. S. Abdel-Khalik, and R. A. Hamdy, "Genetic algorithm based parameter estimation of six-phase induction machine sequence circuits," in *Proc. 2021 22nd IEEE Int. Middle East Power Syst. Conf.*, 2021, pp. 233–238.
[16] M. Ćalasan, M. Micev, Z. M. Ali, A. F. Zobaa, and S. H. Abdel Aleem, "Parameter estimation of induction machine single-cage and double-cage models using a hybrid simulated annealing–evaporation rate water cycle algorithm," *Mathematics*, vol. 8, no. 6, 2020, Art. no. 1024.
[17] S. N. Ipek, M. Taskiran, N. Bekiroglu, and E. Aycicek, "Optimal induction machine parameter estimation method with artificial neural networks," *Elect. Eng.*, vol. 106, no. 2, pp. 1959–1975, 2024.
[18] S. Labdai, L. Chrifi-Alaoui, L. Delahoche, B. Marhic, and P. Bussy, "Hybrid interior point method and genetic algorithm for parameter estimation of three-phase induction motor," in *Proc. IEEE 9th Int. Renewable Sustain. Energy Conf.*, 2021, pp. 1–7.
[19] M. Bansal, A. Goyal, and A. Choudhary, "A comparative analysis of k-nearest neighbor, genetic, support vector machine, decision tree, and long short term memory algorithms in machine learning," *Decis. Analytics J.*, vol. 3, 2022, Art. no. 100071. [Online]. Available: https://www.sciencedirect.com/science/article/pii/S2772662222000261
[20] P. Vas, *Electrical Machines and Drives: A Space-Vector Theory Approach*. Oxford Univ. Press, 1993, pp. 220–661.
[21] E. Levi, "General method of magnetising flux saturation modelling in d–q axis models of double-cage induction machines," *IEE Proc.-Electric Power Appl.*, vol. 144, no. 2, pp. 101–109, 1997.
[22] D. Che, Q. Liu, K. Rasheed, and X. Tao, *Decision Tree and Ensemble Learning Algorithms With Their Applications in Bioinformatics*. H. R. Arabnia and Q.-N. Tran, Eds. New York, NY, USA: Springer New York, 2011, pp. 191–199, doi: 10.1007/978-1-4419-7046-6_19.
[23] I. D. Mienye and N. Jere, "A survey of decision trees: Concepts, algorithms, and applications," *IEEE Access*, vol. 12, pp. 86716–86727, 2024.
[24] O. Sagi and L. Rokach, "Explainable decision forest: Transforming a decision forest into an interpretable tree," *Inf. Fusion*, vol. 61, pp. 124–138, 2020.
[25] R. Shwartz-Ziv and A. Armon, "Tabular data: Deep learning is not all you need," *Inf. Fusion*, vol. 81, pp. 84–90, 2022.
[26] M.-F. Balcan and D. Sharma, "Learning accurate and interpretable decision trees," 2024, *arXiv:2405.15911*.
[27] S. Hara and Y. Yoshida, "Average sensitivity of decision tree learning," in *The Eleventh Int. Conf. Learn. Representations*, 2023.
[28] H. M. Sani, C. Lei, and D. Neagu, "Computational complexity analysis of decision tree algorithms," in *Proc. Artif. Intell. XXXV: 38th SGAI Int. Conf. Artif. Intell.*, Cambridge, U.K., 38. Springer, 2018, pp. 191–197.
[29] R. M. Montgomery, "A comparative analysis of decision trees, neural networks, and Bayesian networks: Methodological insights and practical applications in machine learning," 2024.
[30] K. P. Murphy, *Machine Learning: A Probabilistic Perspective*. Cambridge, MA, USA: MIT Press, 2012.
[31] J. H. Friedman, "Greedy function approximation: A gradient boosting machine," *Ann. Statist.*, vol. 29, no. 5, pp. 1189–1232, 2001.
[32] C.-Y. Lee and E. D. C. Maceren, "Induction motor bearing fault classification using deep neural network with particle swarm optimization-extreme gradient boosting," *IET Electric Power Appl.*, vol. 18, no. 3, pp. 297–311, 2024.
[33] CatBoost, "Overfitting detector in catboost," 2025, Accessed: Feb. 19, 2025. [Online]. Available: https://catboost.ai/docs/en/concepts/overfitting-detector
[34] L. Prokhorenkova, G. Gusev, A. Vorobev, A. V. Dorogush, and A. Gulin, "Catboost: Unbiased boosting with categorical features," pp. 1–234, 2018. [Online]. Available: https://arxiv.org/abs/1706.09516
[35] L. Breiman, "Bagging predictors," *Mach. Learn.*, vol. 24, pp. 123–140, 1996.
[36] G. Dong and H. Liu, *Feature engineering for machine learning and data analytics*. CRC press, 2018.
[37] S. Khalid, T. Khalil, and S. Nasreen, "A survey of feature selection and feature extraction techniques in machine learning," in *Proc. 2014 IEEE Sci. Inf. Conf.*, 2014, pp. 372–378.
[38] J. Cohen, P. Cohen, S. G. West, and L. S. Aiken, *Applied Multiple regression/correlation Analysis for the Behavioral Sciences*. Routledge, 2013.
[39] C. M. Bishop and N. M. Nasrabadi, in *Pattern Recognition and Machine Learning*, 1st ed. (Information Science and Statistics Series). Springer New York, NY: Springer, vol. 1, no. 4, 2006, pp. 1–58.
[40] O. Team, "Optuna: A hyperparameter optimization framework," 2023, Accessed: Feb. 19, 2025. [Online]. Available: https://optuna.org/
[41] S. Watanabe, "Tree-structured parzen estimator: Understanding its algorithm components and their roles for better empirical performance," 2023, *arXiv:2304.11127*.

**EDUARDO FERREIRA RIOS OLIVEIRA** received a technical degree in industrial automation from the Federal Institute of São Paulo (IFSP), São Paulo, Brazil, in 2020. He is currently working toward the undergraduate degree in control and automation engineering with São Paulo State University (UNESP), São Paulo.

He is currently also involved in research as a Scientific Initiation student with São Paulo State University. His research interests include different machine learning approaches such as neural networks and decision tree-based algorithms, three-phase induction motors, and the integration of both fields for innovative solutions in automation and control systems.

**RAFAEL SANTOS** (Member, IEEE) received the B.Sc. degree in control and automation engineering, and the M.Sc. and Ph.D. degrees in electrical engineering from São Paulo State University (UNESP), São Paulo, Brazil, in 2019, 2020, and 2023, respectively.

He is currently an Assistant Professor with São Paulo State University (UNESP), Institute of Science and Technology, Sorocaba. From 2015 to 2016, he made part of his undergraduate studies from Limerick Institute of Technology—Ireland. He has industry experience in the Power Control Business department, Rockwell Automation, where he developed electromechanical projects for motor control centers (MCCs) and electric motor drives. His research interests include industrial electronics and control systems, particularly in: Model predictive control applied to power electronics and energy systems; analysis, design, and implementation of static converters based on impedance networks; control and design of multifunctional inverters for photovoltaic solar energy; analysis, control, and operation of dc and ac electric machines; power quality in electronic energy processing; and integration of energy resources and modernization of offshore energy systems.

Dr. Santos is a Member of the Brazilian Society of Automation (SBA), Brazilian Power Electronics Society (SOBRAEP), and IEEE Power Electronics Society (PELS).

**MARCELO GODOY SIMÕES** (Fellow, IEEE) received the B.Sc. and the M.Sc. degrees from the University of São Paulo, Brazil, in 1985 and 1990, respectively, the Ph.D. degree from The University of Tennessee, USA, in 1995, and the D.Sc. degree (Livre-Docência) from the University of São Paulo in 1998.

He was elevated to the grade of IEEE Fellow, with the citation: "For applications of artificial intelligence in control of power electronics systems." He works for the University of Vaasa, Finland, since 2021, as Professor in flexible and smart power systems. He is a pioneer to apply neural networks and fuzzy logic in power electronics, motor drives, and renewable energy systems. His fuzzy logic-based modeling and control for wind turbine optimization is used as a basis for advanced wind turbine control and it has been cited worldwide. His leadership in modeling fuel cells is internationally and highly influential in providing a basis for further developments in fuel cell automation control in many engineering applications. He made substantial and lasting contribution of artificial intelligence technology in many applications, power electronics and motor drives, fuzzy control of wind generation system, such as Fuzzy Logic-based waveform estimation for power quality, Neural Network-based estimation for vector-controlled motor drives, and integration of alternative energy systems to the electric grid through AI modeling based power electronics control. His current research interests include power electronics, power systems, power quality, smart-grid, and renewable energy systems.

Dr. Simões was an US Fulbright Fellow for AY 2014-15, working for Aalborg University, Institute of Energy Technology (Denmark).

**HELMO MORALES PAREDES** (Senior Member, IEEE) received the B.Sc. degree in electrical engineering from San Agustin National University (UNSA), Arequipa, Peru, in 2002, and the M.Sc. and Ph.D. degrees in electrical engineering from the University of Campinas (UNICAMP), Brazil, in 2006 and 2011, respectively.

He is an Associate Professor with the São Paulo State University (UNESP), Sorocaba, Brazil, since 2011. From 2017 to 2023, he served as the Group of Automation and Integrating Systems (GASI) Leader. In 2009, he was a Visiting Student with the University of Padova, Italy. In 2014, he joined the University of Nottingham in the U.K. as a Visiting Scholar. In 2018, he continued his research abroad as a Visiting Scholar with the Colorado School of Mines, Golden, CO, USA. His research interests include power quality, harmonics propagation, grid-connected converters for renewable energy systems, and microgrid controls.

Dr. Paredes was the recipient of the Prize Paper Award from IEEE TRANSACTIONS ON POWER ELECTRONICS, in 2011, and two consecutive Best Paper Awards from the Brazilian Power Quality Society (SBQEE) in 2021 and 2023, respectively. He is a Member of the Brazilian Power Electronics Society (SOBRAEP) and the Brazilian Automation Society (SBA).